A hybrid twin screw extrusion/electrospinning method to process nanoparticle-incorporated electrospun nanofibres

2008 Nanotechnology 19 165302

(http://iopscience.iop.org/0957-4484/19/16/165302)

Nanotechnology **19** (2008) 165302 (8pp) doi:10.1088/0957-4484/19/16/165302

A hybrid twin screw extrusion/electrospinning method to process nanoparticle-incorporated electrospun nanofibres

Cevat Erisken, Dilhan M Kalyon[1] and Hongjun Wang

Chemical, Biomedical and Materials Engineering Department,
Stevens Institute of Technology, Hoboken, NJ 07030, USA

E-mail: dkalyon@stevens.edu

Received 27 November 2007, in final form 14 February 2008
Published 18 March 2008
Online at stacks.iop.org/Nano/19/165302

Abstract

A new hybrid methodology that fully integrates the processing capabilities of the twin screw extrusion process (conveying solids, melting, dispersive and distributive mixing, pressurization, temperature profiling, devolatilization) with electrospinning is described. The hybrid process is especially suited to the dispersion of nanoparticles into polymeric binders and the generation of nanoparticle-incorporated fibres and nanofibres. The new technology base is demonstrated with the dispersion of β-tricalcium phosphate (β-TCP) nanoparticles into poly(ε-caprolactone) (PCL) to generate biodegradable non-woven meshes that can be targeted as scaffolds for tissue engineering applications. The new hybrid method yielded fibre diameters in the range of 200–2000 nm for both PCL and β-TCP/PCL (35% by weight) composite scaffolds. The degree of crystallinity of polycaprolactone meshes could be manipulated in the 35.1–41% range, using the voltage strength as a parameter. The electrospinning process, integrated with dispersive kneading disc elements, facilitated the decrease of the cluster sizes and allowed the continuous compounding of the nanoparticles into the biodegradable polymer prior to electrospinning. Thermogravimetric analysis (TGA) of the non-woven meshes validated the continuous incorporation of $35 \pm 1.5\%$ (by weight) β-TCP nanoparticles for a targeted concentration of 35%. Uniaxial tensile testing of the meshes with and without the nanoparticles indicated that the ultimate tensile strength at break of the meshes increased from 0.47 ± 0.04 to 0.79 ± 0.08 MPa upon the incorporation of the β-TCP nanoparticles. This demonstration study suggests that the new technology base is particularly suitable for the concomitant dispersion and electrospinning of nanoparticles in the generation of myriad types of functional nanofibres.

1. Introduction

The electrospinning process has been available as a batch method to generate fibres and nanofibres since the 1930s [1–9]. The conventional process typically involves keeping a conductive polymeric solution or melt in a simple cylindrical reservoir, with a plunger on one side and a needle on the other. The needle is attached to an electrical potential source, and the conductive surface facing the needle is grounded. The fibre is drawn as a consequence of the electrical potential, which helps to overcome the surface tension of the droplet that forms at the tip of the needle (the Taylor cone). A whipping unstable motion is typically generated downstream [3, 10–13] to further reduce the diameter of the fibres, possibly into the nano regime. The flow rates are relatively low and are typically in the 1–15 μl min^{-1} range.

The conventional electrospinning process has been applied to generate myriad functional fibres and nanofibres that can be hollow [14, 15], oriented as arrays [16], or converted into ceramics upon pyrolysis [17, 18]. It has also been utilized in other applications including tissue engineering constructs

[1] Author to whom any correspondence should be addressed.

for wound dressing [19], and clothing, filtering, sensing or catalytic membranes [17, 18, 20]. Although the conventional electrospinning process has succeeded in the generation of such novel functional fibres and nanofibres [14–20], it is constricted by its limited capabilities to cover myriad other processing tasks that include handling of solid ingredients, melting, temperature profiling, the blending of polymers, incorporation of additives into a spinning dope, the dispersion of additives and keeping them suspended, removing the air content and changing the concentration of the mixture during processing. The first objective of our study was to develop a new method and apparatus to eliminate these limitations to significantly increase the impact and reach of the electrospinning process.

One particular area that is of high interest currently is the electrospinning of nanofibres that contain functional nanoparticles [21–29]. Especially in the fabrication of sensors [30], filters [31], clothing [32], and scaffolding for tissue engineering tasks, the spinning of nanofibres, which are incorporated with nanoparticles, can offer significant advantages principally due to their very high surface to volume ratios. Such nanoparticle-incorporated nanofibres would, for example, be especially important in the tissue engineering area [33–38]. Another example that could benefit from the reproducible dispersion of nanoparticles into electrospun nanofibres is the controlled release of drug nanoparticles.

The primary objective of any compounding operation aiming to incorporate rigid particles into polymeric binders is the ability to distribute and disperse the rigid particles [39]. This problem becomes more pronounced for the dispersion of nanoparticles including single-walled carbon nanotubes (SWCNTs) [21, 29] and multi-walled carbon nanotubes (MWCNTs) [25, 40, 41]. One principal challenge in the generation of nanoparticle-incorporated nanofibres is the ubiquitous clustering and agglomeration of nanoparticles [42]. Such agglomeration can occur during quiescent or flow conditions and negates the advantages offered by the very high surface to volume ratios of nanoparticles. It is evident that the conventional electrospinning process has no capabilities to disperse nanoparticles into polymer melts or solutions, to keep them suspended, and to prevent their agglomeration in a predictable and reproducible manner over the long durations necessary for electrospinning. Thus, the second objective of our investigation was to demonstrate the new method and apparatus for the dispersion of nanoparticles to generate nanoparticle-incorporated nanofibres. This demonstration was accomplished via the dispersion of nanoparticles of β-tricalcium phosphate, β-TCP, widely used, for example, in the bone generation area, into a solution of biodegradable poly(ε-caprolactone), PCL, which is again widely used in various tissue engineering applications, within the confines of a single integrated process. As described next, a family of non-woven PCL/β-TCP meshes (with differing crystallinity, hydrophilicity, pore size, fibre diameter and a wide range of mechanical properties) could be obtained to demonstrate the utility of the hybrid process.

2. Experimental details

2.1. Materials

The polycaprolactone (PCL), with a number average molecular weight of 80 000, and β-tricalciumphosphate (β-TCP) nanoparticles were procured from Sigma-Aldrich. The dichloromethane (DCM) solvent was obtained from Pharmco.

2.2. The hybrid twin screw extrusion/electrospinning (TSEE) process

The schematics and the basic apparatus of the hybrid twin screw extrusion/electrospinning (TSEE) process are shown in figure 1. The process principally consists of a twin screw extruder with fully intermeshing and co-rotating screws of 7.5 mm diameter (available from Material Processing and Research, Inc., Hackensack, NJ) integrated with a spinneret die with multichannels for flow and shaping, and connected to a high-voltage supply (ES30P-5W, Gamma High Voltage Research Inc., Ormond Beach, FL) that is capable of generating DC voltages up to 30 kV. Injection ports and other feed ports in the barrel enable the introduction of the liquid and solid ingredients/additives simultaneously and continuously. All of the tooling, including the barrel and die sections, is splittable to allow access to the samples as they exist during processing. The screw sections can be configured to allow different operations like conveying, melting, mixing, shaping, and devolatilization to occur simultaneously. The dispersive mixing capability of the screws can also be tailored by using combinations of kneading discs with fully flighted elements, staggered at the desired stagger angle and direction (kneading discs) or at any pitch (fully flighted screw elements). The continuous nature of the process is a major advantage and enables manufacture over long durations on a reproducible basis, to thus eliminate one of the major drawbacks of the conventional electrospinning process. To our knowledge the combination of extrusion with electrospinning has been tried only once (using single screw extrusion) but suffered from the fundamental limitations of the single screw extrusion process on the one hand and the mismatch between the processing rate in the extruder and the electrospinning process on the other [43].

The special design feature of the screws is the availability of reversely configured kneading blocks, i.e., lenticular discs staggered at an angle, to enable the application of relatively high shearing stresses to the break-up of agglomerates of nanoparticles, a feature totally lacking in the conventional electrospinning process where the solution is mechanically displaced with a plunger/ram. The presence of tight clearances between the screws and the barrel, and between the screws, contributes to the dispersion capability of the process during conveying/melting/pumping/devolatilization, where the dispersive mixing and associated break-up of the agglomerates arise due to the repeated passage of the suspension through small gaps, where relatively high shearing stresses are applied. The fully intermeshing and self-swiping features of the co-rotating screws facilitate further distributive mixing of the ingredients.

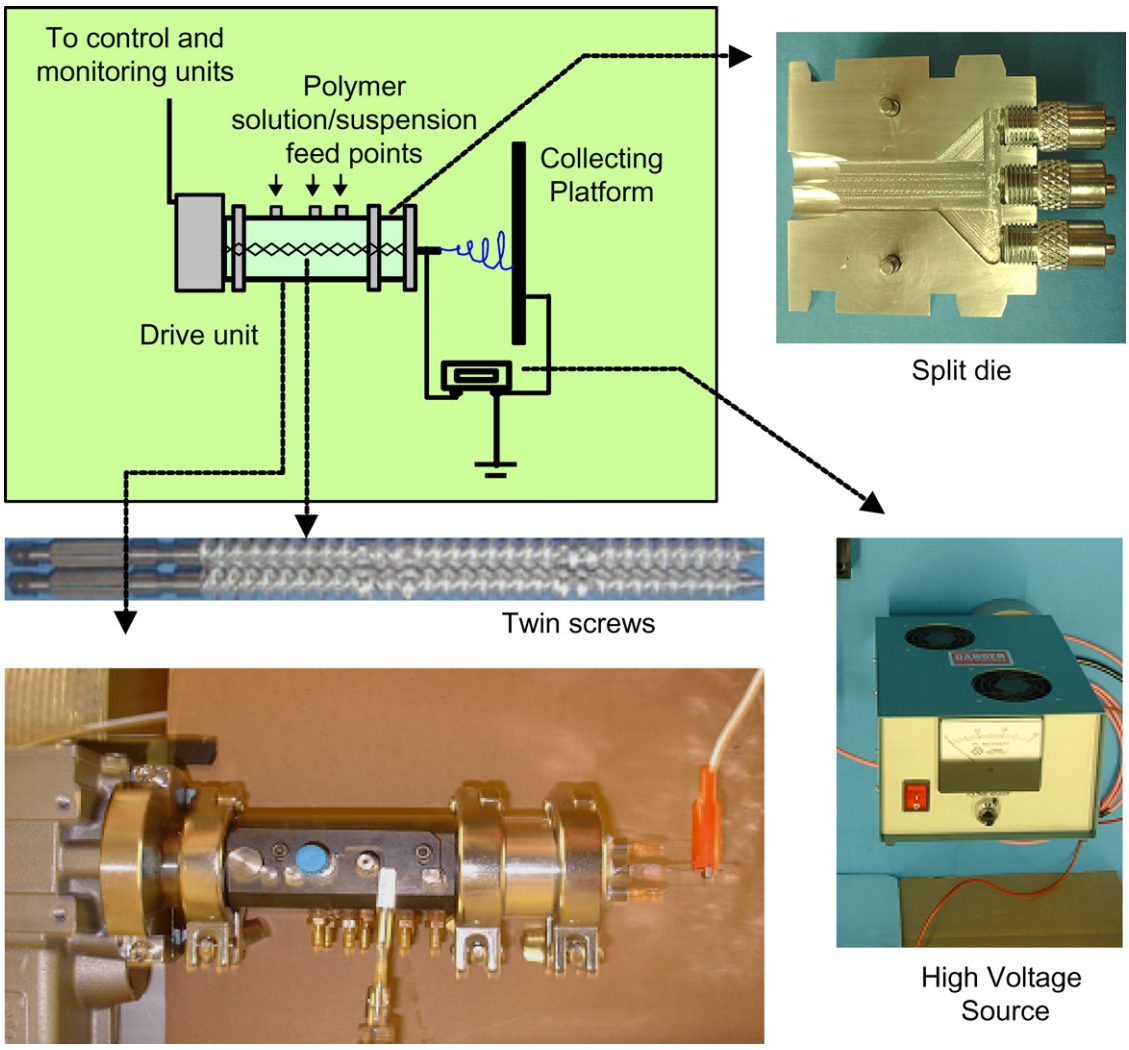

Figure 1. Schematics and the apparatus of the twin screw extrusion/electrospinning (TSEE) process for the generation of nanoparticle-incorporated nanofibres (not to scale). The split die was designed/manufactured with multiple apertures to allow multiple fibres, but only one aperture was used in this study.

(This figure is in colour only in the electronic version)

The operation of the twin screw extruder (dual drive, i.e., could be hydraulically or servo driven) was controlled by the aid of a computerized field-point based data acquisition/process control system. The unit has the capability to control temperatures over three different and separate heat transfer zones, which is again not possible in conventional electrospinning. The drive and the barrel/die units of the extruder were built to be amenable for electrical insulation. Furthermore, non-conducting bolts and nuts were used for connecting the units, again for electrical insulation. The screw configuration was selected to generate three consecutive mixing zones, two of which were sealed with reversely staggered kneading discs and the third sealed with the die, to generate partially full sections in the extruder. This enables the breakdown of the continuity of the feed streams at intervals, and thus prevents the charges from reaching relatively long distances.

The polycaprolactone was dissolved in dichloromethane (DCM) at a ratio of 12/100 (g ml^{-1}). The PCL/DCM solution was fed into the first mixing zone of the extruder where β-TCP nanoparticles were also introduced to generate a β-TCP/PCL ratio of 35/65 by weight (16/84 by volume). Two different sets of demonstration experiments were performed. In the first part, only the PCL-DCM solution was processed and the processing conditions were altered systematically to determine the optimal conditions to obtain a non-woven mesh of fibres and nanofibres collected continuously on the grounded plate. In these experiments the distance between the tip of the spinneret and the collecting plate, the applied potential difference, the inner spinneret diameter and the feed rate of the solution were altered systematically between 5 and 10 cm, 5 and 10 kV, 0.25 and 0.60 mm and 1 and 15 $\mu l\,min^{-1}$, respectively. In the second set of experiments, the compositions of the formulations, i.e., the feed rates of the PCL-DCM solution and PCL-β-TCP-DCM suspension, were varied in order to obtain non-woven meshes with differing β-TCP nanoparticle concentrations.

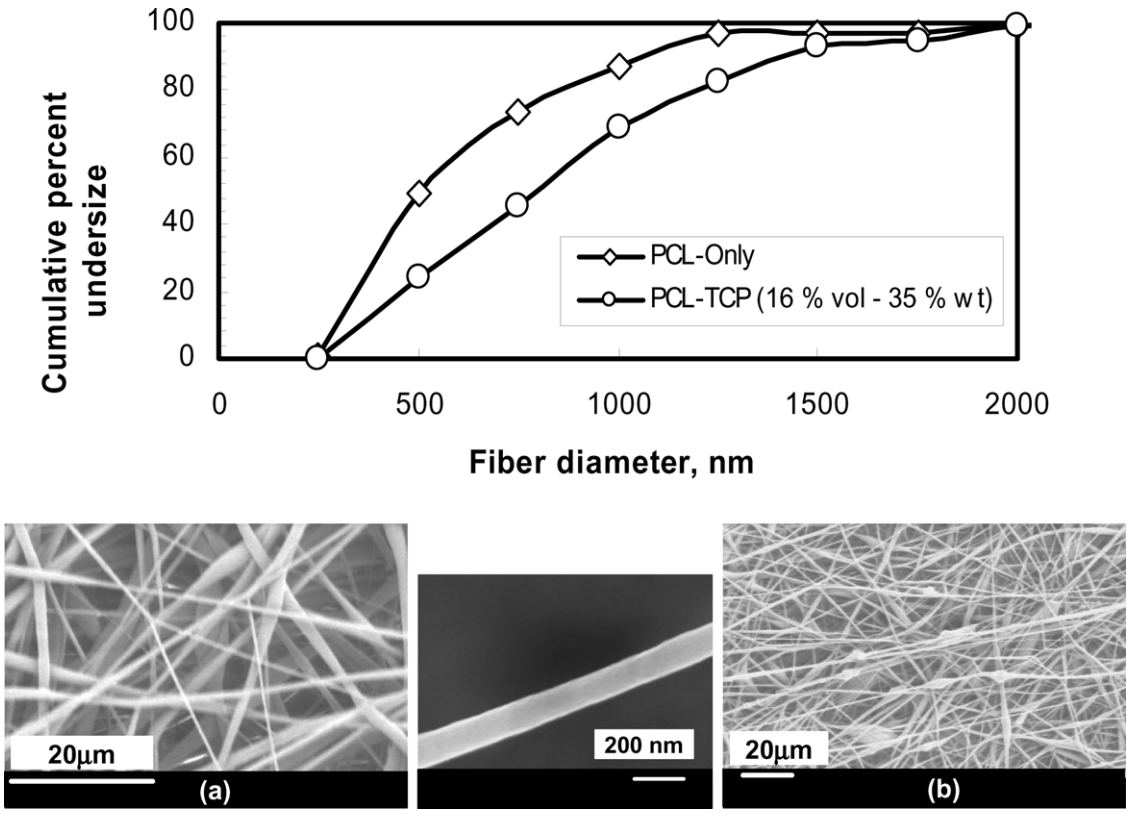

Figure 2. Fibre diameter distribution and SEM images of electrospun (a) PCL only and (b) PCL-β-TCP meshes for one set of operating parameters (applied potential = 5 kV, distance = 7.5 cm, flow rate = 10 μl min^{-1}, spinneret inner diameter = 0.6 mm).

2.3. Characterization

The linear viscoelastic properties of the PCL-DCM polymer solution were characterized using a Rheometric Scientific ARES rheometer (Rheometrics, NJ). A differential scanning calorimeter (DSC-Q100, TA Instruments, USA) was used for measurement of the bulk crystallinity of the fibres under N_2 using a heating rate of 10 °C min^{-1}. The degree of crystallinity was determined from the ratio of the heat of fusion of the PCL to that of pure crystalline PCL, which is specified as 139.5 J g^{-1} [44]. The porosity of the electrospun meshes was determined by using their apparent densities. The diameter, shape and surface properties of the electrospun fibres were documented using a LEO Gemini 982 scanning electron microscope. The weight fraction of β-TCP contained in electrospun PCL-β-TCP non-woven meshes was validated by using a thermogravimetric analysis apparatus (TGA-Q50, TA Instruments) upon heating from 25 to 550 °C at 15 °C min^{-1} under N_2.

The x-ray diffraction analysis of electrospun PCL and PCL-[β-TCP] composite meshes was performed using a Rigaku/Miniflex$^+$ diffractometer. Cu K_α radiation (run at 15 mA and 30 kV) was used. The samples were scanned in the Bragg angle (2θ) range of 25°–37° at a scan rate of 1° min^{-1}, with a sampling interval of 0.04°. The tensile properties of PCL and PCL-β-TCP composite meshes with surface areas of 25 mm by 7.5 mm were characterized using a Rheometrics dynamic mechanical analyser at a cross-head speed of 0.01 mm min^{-1} under ambient conditions.

The contact angles of the PCL and PCL-β-TCP composite meshes were measured using a goniometer in conjunction with the sessile drop method. Specifically, 10 μl of deionized water droplet was placed on the surface of meshes and imaged within 5 s using Sony-DVgate imaging software. The contact angles were measured using Scion Image software.

3. Results and discussion

The linear viscoelastic properties of the PCL-DCM polymer solution (9.5% by volume or 8.3% by weight) were characterized and the storage modulus, loss modulus and the magnitude of complex viscosity values of PCL/DCM solutions ranged between 1.4 Pa and 617.6 Pa, 8.7 Pa and 375.3 Pa, and 8.9 Pa s and 722.6 Pa s, respectively for the PCL concentration range of 8.3%–9.1% by weight (9.5%–10.3% by volume), at 1 rps and 24 °C.

The application of the hybrid technology solely to the feeding/conveying, pressurization, temperature control and electrospinning of the PCL/DCM solutions generated nanofibres and fibres in the range of 200–2000 nm, as shown in figure 2. The crystallinity of such polymeric meshes is important vis-à-vis their mechanical properties as well as their permeability, biodegradability in controlled drug release applications, and biodegradability and cellular response in tissue engineering [45]. The non-woven mesh shown in figure 2(a) exhibited crystallinity values of 41.0%, 35.2% and 35.1% at the applied voltage strengths of 0.7 kV cm^{-1},

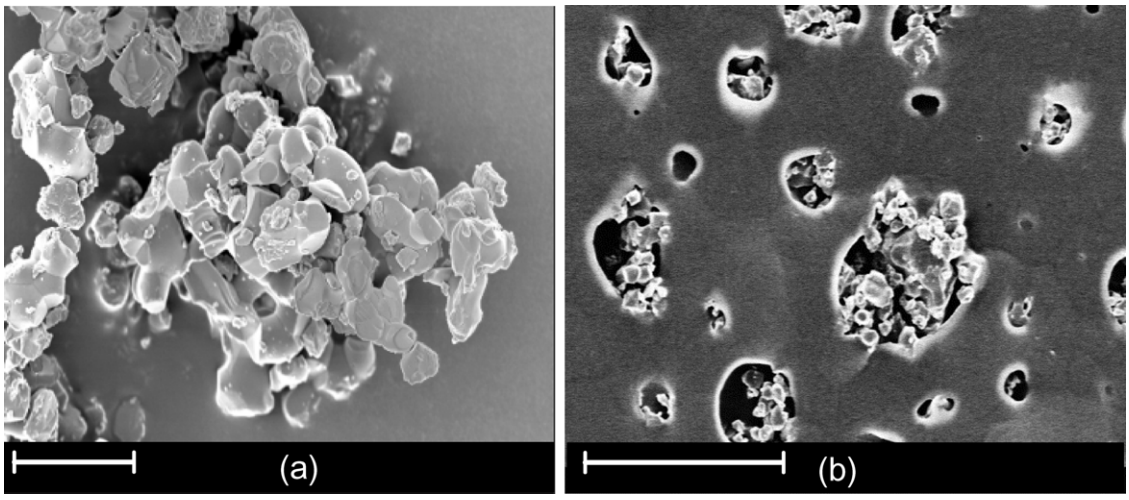

Figure 3. Agglomerates of β-TCP nanoparticles prior to the processing in the twin screw extrusion/electrospinning (TSEE) process. (a) β-TCP nanoparticles (the scale bar is 5 μm), (b) PCL-β-TCP suspension prior to dispersion (the scale bar is 20 μm).

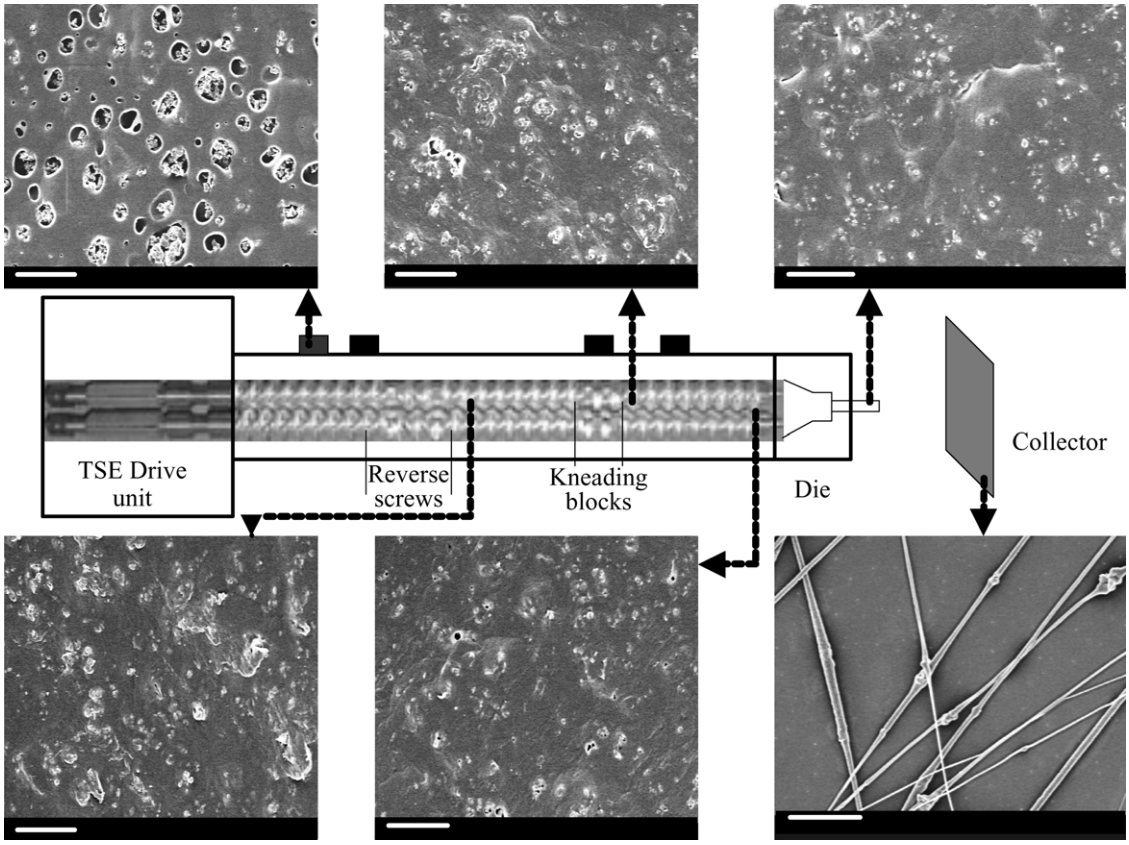

Figure 4. Deagglomeration of nanoparticles at different stages of continuous processing (the scale bar is 20 μm).

1.0 kV cm^{-1} and 1.3 kV cm^{-1}, respectively; thus the process could reduce the degree of crystallinity of PCL from its pre-processing degree of crystallinity of 42.0%. The decrease of the fibre diameter with increasing voltage strength increased the rate of evaporation of the solvent and decreased the crystallinity of PCL. The melting temperature of the PCL (the highest temperature at which the last trace of crystallinity is observed) decreased slightly from 68 to 66.5 °C as the voltage strength increased from 0.7 to 1.3 kV cm^{-1}.

For many applications, including filtering, sensing or tissue engineering, it is important to keep the pore size within a narrow range, and the typical pore sizes for the PCL non-woven meshes (shown in figure 2) could be kept within the 5–50 μm range. This range would be particularly suitable for cartilage and skin tissue applications [46, 47]. Similarly,

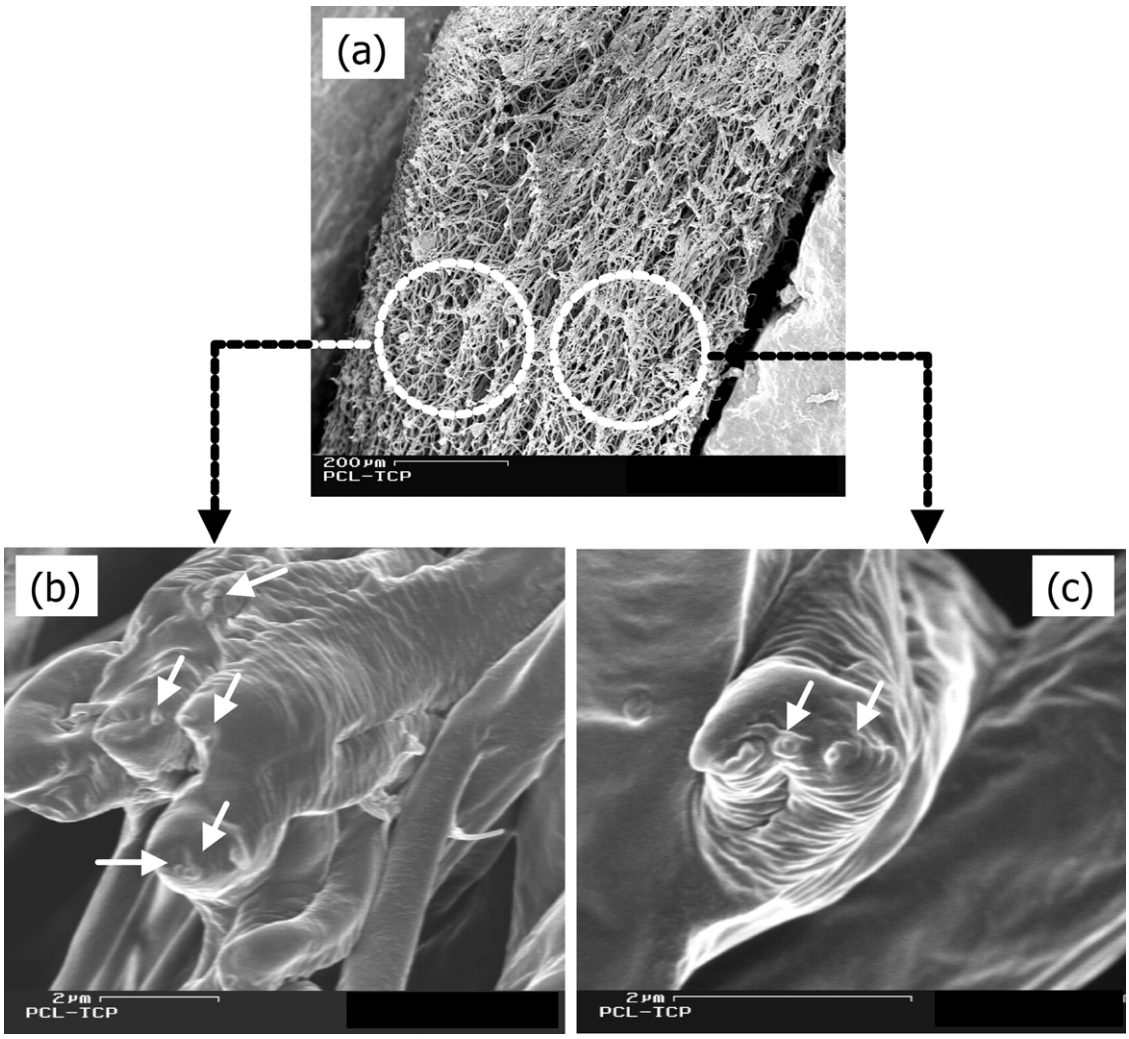

Figure 5. β-TCP nanoparticles within the bulk of PCL fibres (the scale bars are 200 μm in (a), 2 μm in (b), and 2 μm in (c)).

the 87 $\pm$ 2% porosity of PCL meshes can be considered to be appropriate for cartilage tissue applications [48]. The concentrations of the β-TCP in PCL were varied in the range of 20–40% by weight. The β-TCP is generally only available as nanoparticle agglomerates that are in the 2.5–20 μm range, as shown in figure 3. The ultimate β-TCP nanoparticles are in the 100–2500 nm range in the powder.

Figure 4 shows the scanning electron micrographs of β-TCP nanosuspensions prior to being fed into the twin screw extrusion/electrospinning process and at different locations within the confines of the extruder, as collected upon a dead stop from the steady state. The decrease of the nanoparticle cluster sizes upon the dispersive mixing in the twin screw extruder as a function of distance in the downchannel direction is clearly shown. The kneading discs of the twin screw extruder allow the compounding of the nanoparticles into the polymeric binder on the one hand and facilitate the decrease of the cluster sizes, making the subsequent spinning of fibres possible on the other. The cross section of the PCL-β-TCP non-woven mesh and the typical distributions of β-TCP nanoparticles within the bulk of PCL fibres are shown in figure 5. As seen here, the β-TCP nanoparticles appear to be non-preferentially distributed, but unfortunately we did not have the means to characterize the statistics of such spatial distributions of the nanoparticles within the volume of the electrospun fibres/nanofibres.

The β-TCP nanoparticle contents of the fibres were validated using TGA, which generated a range of 35 $\pm$ 1.5% β-TCP at the targeted 35% by weight condition. The stability of the β polymorph of the β-TCP upon processing and the concentration of the β-TCP nanoparticles were verified using wide-angle x-ray diffraction (figure 6).

Typical nominal stress (normal force over the initial cross-sectional area) versus the strain data obtained upon tensile deformation of the non-woven mesh samples with and without β-TCP are shown in figure 7. The strain limit of elasticity for both PCL-only and PCL-β-TCP composite meshes was 10% strain. This was followed by a ductile deformation to reach an ultimate tensile strength at break of 0.47 $\pm$ 0.04 MPa and 0.79 $\pm$ 0.08 MPa, for PCL-only and PCL-β-TCP composite meshes, respectively. The Young's modulus and the elongation at break values of PCL-only and PCL-β-TCP meshes were 10.5 kPa and 18.3 kPa, and 342 $\pm$ 24% and 130 $\pm$ 18%, respectively. Further changes in the mechanical properties can be achieved by further tailoring of the processing geometries

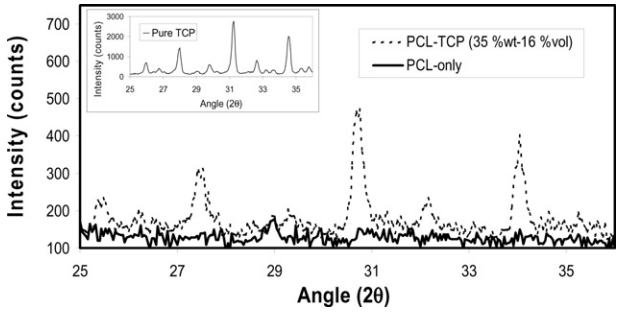

Figure 6. XRD scan of PCL-only and PCL-β-TCP nanocomposite electrospun meshes.

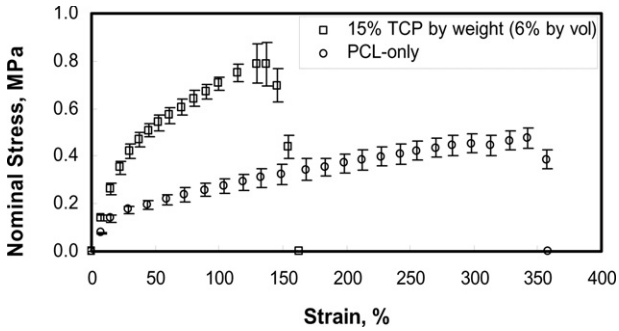

Figure 7. Stress–strain behaviour of PCL-only and PCL-β-TCP nanocomposite meshes (error bars determined at the $\alpha = 0.05$ level).

and conditions to achieve differing degrees of dispersion and mixedness and particle size distributions.

The tensile strengths at break values of the PCL and PCL/β-TCP constructs are 0.47 and 0.79 MPa, respectively. The hybrid TSEE process would be especially suitable for the manufacture of bizonal or multi-zonal constructs with different mechanical properties at opposing sides, say one zone (PCL-only) with greater elongation at break that enables it to stretch without damaging the other zone containing β-TCP nanoparticles, without the need to interrupt the process simply by changing the respective flow rates with time.

Another interesting aspect of the incorporation of β-TCP nanoparticles is the change in the wettability of the non-woven meshes. Surface contact angles of PCL and PCL-β-TCP composite meshes were measured using a goniometer in conjunction with the sessile drop method. The incorporation of β-TCP ceramic nanoparticles into PCL decreases the contact angle upon the increase of the surface energy (figure 8), consistent with earlier studies [49]. The ability to change the wettability as a result of different β-TCP concentrations in PCL again provides the capability of forming different zones with varying contact angles in a single nanocomposite construct.

4. Conclusions

Overall, we have developed and demonstrated an integrated method and apparatus for the dispersion of nanoparticles into a polymeric binder and the generation of electrospun nanofibres

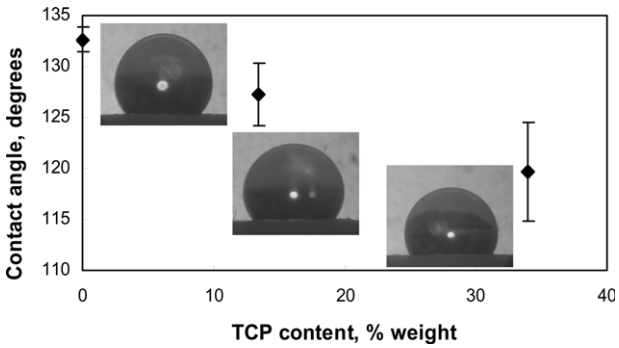

Figure 8. Contact angles measured on non-woven electrospun meshes containing different β-TCP nanoparticle concentrations.

and fibres from the resulting compound within the confines of the same process, i.e., the twin screw extrusion/electrospinning process. The process allows the compounding of various additives including nanoparticles with a high degree of freedom not found in the conventional electrospinning process along with enabling additional processing steps including melting of the polymer and devolatilization within the confines of a single integrated process. The process should offer significant new advantages in myriad industries that utilize nanoparticle-incorporated fibres and nanofibres.

Acknowledgments

We are grateful to Material Processing & Research Inc. of Hackensack, NJ for making their MPR 7.5 mm twin screw extrusion platform available to us free of charge and for the help that they have provided over the course of the project. We thank Dr H Gevgilili of HFMI for his contributions to the development and implementation of the hybrid technology.

References

[1] Fromhals A 1934 *US Patent Specification* 1975504
[2] Baumgarten P K 1971 *J. Colloid Interface Sci.* **36** 71
[3] Hohman M M, Shin M, Rutledge G and Brenner M P 2001 *Phys. Fluids* **13** 2201
[4] Deitzel J M, Kleinmeyer J, Harris D and Tan B N C 2001 *Polymer* **42** 261
[5] Demir M M, Yilgor I, Yilgor E and Erman B 2002 *Polymer* **43** 3303
[6] Huang Z M, Zhang Y Z, Kotaki M and Ramakrishna S 2003 *Comput. Sci. Technol.* **63** 2223
[7] Frenot A and Chronakis I S 2003 *Curr. Opin. Colloid Interface Sci.* **8** 64
[8] Li D and Xia Y 2004 *Adv. Mater.* **16** 1151
[9] Teo W E and Ramakrishna S 2006 *Nanotechnology* **17** 89
[10] Reneker D H, Yarin A L, Fong H and Koombhongse S 2000 *J. Appl. Phys.* **87** 4531
[11] Doshi J and Reneker D H 1995 *J. Electrost.* **35** 151
[12] Yarin A L, Koombhongse S and Reneker D H 2001 *J. Appl. Phys.* **89** 3018
[13] Fridrikh S V, Yu J H, Brenner M P and Rutledge G C 2003 *Phys. Rev. Lett.* **90** 144502
[14] Li D and Xia Y 2004 *Nano Lett.* **4** 933
[15] McCann J T, Li D and Xia Y 2005 *J. Mater. Chem.* **15** 735
[16] Kameoka J and Craighead H G 2003 *Appl. Phys. Lett.* **83** 371

[17] Li D and Xia Y 2003 *Nano Lett.* **3** 555
[18] Yang Q B, Li D M, Hong Y L, Li Z Y, Wang C, Qiu S L and Wei Y 2003 *Synth. Met.* **137** 973
[19] Min B M, Lee G, Kim S H, Nam Y S, Lee T S and Park W H 2004 *Biomaterials* **25** 1289
[20] Bowlin G L, Simpson D G and Wnek G 2003 *US Patent Specification* 20030207638
[21] Ko F, Gogotsi Y, Ali A, Naguib N, Ye H, Yang G L, Li C and Willis P 2003 *Adv. Mater.* **15** 1161
[22] Pedicini A and Farris R J 2004 *J. Polym. Sci. B Polym. Phys.* **42** 752
[23] Dharmaraj N, Park H C, Lee B M, Viswanathamurthi P, Kim H Y and Lee D R 2004 *Inorg. Chem. Commun.* **7** 431
[24] Wutticharoenmongkol P, Sanchavanakit N, Pavasant P and Supaphol P 2006 *Macromol. Biosci.* **6** 70
[25] Dror Y, Salalha W, Khalfin R L, Cohen Y, Yarin A L and Zussman E 2003 *Langmuir* **19** 7012
[26] Kearns J C and Shambaugh R L 2002 *J. Appl. Polym. Sci.* **86** 2079
[27] Kikuchi M, Koyama Y, Yamada T, Imamura Y, Okada T, Shirahama N, Akita K, Takakuda K and Tanaka J 2004 *Biomaterials* **25** 5979
[28] Li X, Yao C, Sun F, Song T, Li Y and Pu Y 2008 *J. Appl. Polym. Sci.* **107** 3756
[29] Salalha W, Dror Y, Khalfin R L, Cohen Y, Yarin A L and Zussman E 2004 *Langmuir* **20** 9852
[30] Wang X, Kim Y-G, Drew C, Ku B-C, Kumar J and Samuelson L A 2004 *Nano Lett.* **4** 331
[31] Hajra M G, Mehta K and Chase G G 2003 *Sep. Purif. Technol.* **30** 79
[32] Klein E 2000 *J. Membr. Sci.* **179** 1
[33] Jin H J, Fridrikh S V, Rutledge G C and Kaplan D L 2002 *Biomacromolecules* **3** 1233
[34] Matthews J A, Wnek G E, Simpson D G and Bowlin G L 2002 *Biomacromolecules* **3** 232
[35] Yoshimoto H, Shin Y M, Terai H and Vacanti J P 2003 *Biomaterials* **24** 2077
[36] Huang Z M, Zhang Y Z, Ramakrishna S and Lim C T 2004 *Polymer* **45** 5361
[37] Li M, Mondrinos M J, Gandhi M R, Ko F K, Weiss A S and Lelkes P I 2005 *Biomaterials* **26** 5999
[38] Fujihara K, Kotaki M and Ramakrishna S 2005 *Biomaterials* **26** 4139
[39] Lozano T, Lafleur P G and Grmela M 2002 *Can. J. Chem. Eng.* **80** 1135
[40] Kim G-M, Michler G H and Potschke P 2000 *Polymer* **46** 7346
[41] Ge J J, Hou H, Li Q, Graham M J, Greiner A, Reneker D H, Harris F W and Cheng S Z D 2004 *J. Am. Chem. Soc.* **126** 15754
[42] Yeo L Y and Friend J R 2006 *J. Exp. Nanosci.* **1** 177
[43] Lyons J, Li C and Ko F 2004 *Polymer* **45** 7597
[44] Pitt C G, Chasalow F I, Hibionada Y M, Klimas D M and Schindler A 1981 *J. Appl. Polym. Sci.* **26** 3779
[45] Mochizuki M and Hirami M 1997 *Polym. Adv. Technol.* **8** 203
[46] Griffon D J, Sedighi M R, Schaeffer D V, Eurell J A and Johnson A L 2006 *Acta Biomater.* **2** 313
[47] Zeltinger J, Sherwood J K, Graham D A, Mueller R and Griffith L G 2001 *Tissue Eng.* **7** 557
[48] Setton L A, Elliott D M and Mow V C 1999 *Osteoarthr. Cartil.* **7** 2
[49] Zhou Y, Hutmacher D W, Varawan S L and Lim T M 2007 *Polym. Int.* **56** 333